



## Power Coupling between Step-Index Optical Fiber Sections with Different Refractive Indices

*Mohamed A. Abdulalim, Khalid F. Hussein, and Fatma M. Elhefnawi*  
*Electronics Research Institute, Cairo, Egypt.*

[abo\\_safe@hotmail.com](mailto:abo_safe@hotmail.com) , [khalid\\_fawzy@hotmail.com](mailto:khalid_fawzy@hotmail.com) , [fatma\\_hefnawi@hotmail.com](mailto:fatma_hefnawi@hotmail.com)

### Abstract

In this paper, the guided modes as well as the radiation modes for step index optical fibers are obtained. The problem of scattering of a dominant guided mode in an optical fiber section due to a step transition to another fiber section of different refractive index is treated rigorously using the mode-matching technique. This technique employs the complete spectrum of modes and results in a system of singular integral equations. Using a numerical method that accounts for the kernel singularities, the system of singular integral equations is converted into a finite system of linear equations, which is amenable for exact numerical solution. The radiation power due to the discontinuity as well as the power coupled to the second fiber section are evaluated. The power balance is verified, where the summation of the reflected and radiated power together with that coupled to the second fiber section are found equal to the power of the incident mode.

### 1. Introduction

A significant factor in any optical fiber system installation is the interconnection of fiber sections in low-loss manner. Since the optical power that can be coupled from one fiber to another is limited by the number of modes that can propagate in each fiber [1], the discontinuity losses in the single-mode optical fiber is more dangerous than that of the multi-mode optical fiber. The discontinuities along an optical fiber can be classified into three categories. The first is the mechanical misalignment, which may be longitudinal, lateral, and/or angular misalignment. The second is the geometrical discontinuity, which results from the core diameter mismatch. The third is the differences in waveguide characteristics such as, the numerical aperture and core refractive-index-profile mismatches [1].

Numerous techniques exist for analyzing optical waveguide systems that have axial discontinuities. The methods of analysis of optical waveguide discontinuities can be classified as modal and non-modal methods. Non-modal methods of analysis do not employ a modal representation of the optical field. One of the non-modal methods is the beam propagation method (BPM). Like the non-modal methods of analysis, the standard (BPM) gives only information about the total optical field but fails to give a physical insight of the obtained results. Moreover, this method is only efficient for weakly guiding structures presenting small deviation angle and having no polarization dependence. Modal methods of analysis are based on the decomposition of the total optical field into local guided and radiation modes, thus giving physical insight of the problem in view of the modal components and overcoming most of the limitations of the non-modal methods. The mode-matching technique is the most common among the modal methods of analysis used for treating discontinuity problems along the optical fiber.

Like all dielectric waveguides the optical fiber supports a finite number of guided modes, which is supplemented by an infinite continuum of unguided radiation modes [2]. The electromagnetic fields in the optical fiber can be completely represented by employing these two sets of modes. The guided modes describe the propagation of light along nonabsorbing optical waveguides in region sufficiently far from any source of excitation, where the spatial steady state is reached but the radiation modes describe the spatial transient, due to discontinuities, or any other irregularities along the waveguide [3].



The guided modes of step-index optical fibers are treated in many publications [4]. The radiation modes of optical fibers were obtained in [3] considering infinite radius of the cladding. The method of characteristic phase shifts [5] is employed in the present work to get the radiation modes of the finite cladding optical fiber. The radiation modes are orthogonal to each other with respect to the mode order as well as the radial propagation constant. The two sets of modes (guided and radiation) are also orthogonal to each other.

In the present work, the problem of power coupling between two single-mode optical fiber sections with different refractive indices is analyzed using the mode-matching technique. The dominant guided mode of the first fiber section carrying a unity power is assumed incident on the discontinuity plane. The fields reflected back to the first section as well as those transmitted to the second fiber section are expanded in terms of the complete set of modes of the corresponding fiber section with unknown excitation coefficients. The transverse fields are matched on the two sides of the discontinuity plane resulting in a system of singular integral equations. A numerical method that accounts for the kernel singularities is used to convert the system of singular integral equations into a finite system of linear equations, which is amenable for exact numerical solution.

The power loss due to the discontinuity as well as the power coupled to the second section are evaluated. To verify the validity of the obtained results the power balance is investigated, where the power loss together with that coupled to the second fiber section should be equal to the power of the incident wave.

## 2. The Complete set of modes of the step-index optical fiber

The complete set of modes of the optical fiber consists of guided modes and radiation modes. The guided modes of the step-index optical fiber are treated in many publications [1], [2], [3], [4]. The radiation modes can be obtained by using the characteristic phase shifts method [5].

### 2.1. Radiation modes of the step-index optical fiber

The radiation fields in the optical fiber surroundings and in the far zone cannot be represented by the guided modes alone. The spectrum of such an open waveguide should be completed by adding the continuous spectrum of modes. Such modes may be excited by sources or irregularities in the open optical fiber waveguides [6]. The continuous spectrum of modes can be derived from the solution of the Helmholtz equation having oscillatory rather than exponentially decaying character at the large transverse distance [7]. Thus the radiation mode is a standing wave in the radial direction, and hence it is expressed as a summation of incoming (incident) and outgoing (reflected) cylindrical waves in the radial direction in the air region [7].

The mode field, which is the sum of both incident and reflected fields, can be expressed as

#### i. Air fields ( $r \geq b$ )

$$E_z^a = \eta_0 e_n^a W_n(kr, \alpha_n) \cos n\phi \quad (1-a)$$

$$H_z^a = h_n^a W_n(kr, \alpha_n) \sin n\phi \quad (1-b)$$

$$H_r^a = \frac{-j}{k^2} \left[ \beta k h_n^a W_n'(kr, \alpha_n) + \frac{n \omega \epsilon_0}{r} \eta_0 e_n^a W_n(kr, \alpha_n) \right] \sin n\phi \quad (1-c)$$

$$H_\phi^a = \frac{-j}{k^2} \left[ \frac{n\beta}{r} h_n^a W_n(kr, \alpha_n) + \omega \epsilon_0 k \eta_0 e_n^a W_n'(kr, \alpha_n) \right] \cos n\phi \quad (1-d)$$

$$E_r^a = \frac{-j}{k^2} \left[ \beta \eta_0 k e_n^a W_n'(kr, \alpha_n) + \frac{n \omega \mu}{r} h_n^a W_n(kr, \alpha_n) \right] \cos n\phi \quad (1-e)$$



$$E_{\phi}^a = \frac{-j}{k^2} \left[ \frac{-n\beta}{r} \eta_0 e_n^a W_n(kr, \alpha_n) - \omega k \mu h_n^a W_n'(kr, \alpha_n) \right] \sin n\phi \quad (1-f)$$

where

$$W_n(kr, \alpha_n) = \frac{1}{2} \left[ \exp^{-j\alpha_n} H_n^{(2)}(kr) + \exp^{j\alpha_n} H_n^{(1)}(kr) \right] \quad (2-a)$$

An alternative expression for  $W_n(kr, \alpha_n)$  is given as

$$W_n(kr, \alpha_n) = J_n(kr) \cos \alpha_n - Y_n(kr) \sin \alpha_n \quad (2-b)$$

ii. Core fields ( $r \leq a$ )

$$E_z^c = e_n^c \eta_c J_n(k_1 r) \cos n\phi \quad (3-a)$$

$$H_z^c = h_n^c J_n(k_1 r) \sin n\phi \quad (3-b)$$

$$H_r^c = \frac{-j}{k_1^2} \left[ \beta k_1 h_n^c J_n'(k_1 r) + n \frac{\omega \varepsilon_c}{r} \eta_c e_n^c J_n(k_1 r) \right] \sin n\phi \quad (3-c)$$

$$H_{\phi}^c = \frac{-j}{k_1^2} \left[ \frac{n\beta}{r} h_n^c J_n(k_1 r) + \omega \varepsilon_c k_1 \eta_c e_n^c J_n'(k_1 r) \right] \cos n\phi \quad (3-d)$$

$$E_r^c = \frac{-j}{k_1^2} \left[ \beta k_1 \eta_c e_n^c J_n'(k_1 r) + \frac{n\omega \mu}{r} h_n^c J_n(k_1 r) \right] \cos n\phi \quad (3-e)$$

$$E_{\phi}^c = \frac{-j}{k_1^2} \left[ \frac{-n\beta}{r} \eta_c e_n^c J_n(k_1 r) - \omega \mu k_1 h_n^c J_n'(k_1 r) \right] \sin n\phi \quad (3-f)$$

iii. Cladding fields ( $a \leq r \leq b \rightarrow \infty$ )

$$E_z^d = \eta_d [C_j J_n(k_2 r) + C_y Y_n(k_2 r)] \cos n\phi \quad (4-a)$$

$$H_z^d = [D_j J_n(k_2 r) + D_y Y_n(k_2 r)] \sin n\phi \quad (4-b)$$

$$H_r^d = \frac{-j}{k_2^2} \left[ \beta k_2 [D_j J_n'(k_2 r) + D_y Y_n'(k_2 r)] + \frac{n\omega \varepsilon_d}{r} \eta_d [C_j J_n(k_2 r) + C_y Y_n(k_2 r)] \right] \sin n\phi \quad (4-c)$$

$$H_{\phi}^d = \frac{-j}{k_2^2} \left[ \frac{n\beta}{r} [D_j J_n(k_2 r) + D_y Y_n(k_2 r)] + \omega \varepsilon_d k_2 \eta_d [C_j J_n'(k_2 r) + C_y Y_n'(k_2 r)] \right] \cos n\phi \quad (4-d)$$

$$E_r^d = \frac{-j}{k_2^2} \left[ \beta \eta_d k_2 [C_j J_n'(k_2 r) + C_y Y_n'(k_2 r)] + \frac{n\omega \mu}{r} [D_j J_n(k_2 r) + D_y Y_n(k_2 r)] \right] \cos n\phi \quad (4-e)$$

$$E_{\phi}^d = \frac{-j}{k_2^2} \left[ \frac{-n\beta}{r} \eta_d [C_j J_n(k_2 r) + C_y Y_n(k_2 r)] - \omega \mu k_2 [D_j J_n'(k_2 r) + D_y Y_n'(k_2 r)] \right] \sin n\phi \quad (4-f)$$



where  $\mu$ ,  $\epsilon_0$  and  $\eta_0$  are permeability, permittivity, and wave impedance of free space, respectively,  $\eta_c$  and  $\eta_d$  are the core and cladding wave impedances, respectively,  $n$  is the mode order,  $\omega$  is the angular frequency,  $r$ ,  $\phi$  and  $z$  are the cylindrical coordinates.  $e_n^a, h_n^a, e_n^c, h_n^c, C_j, C_y, D_j$  and  $D_y$  are unknowns to be determined.  $J_n(k_1 r)$  is the Bessel function of first kind,  $Y_n(k_2 r)$  is the Bessel function of second kind,  $H_n^{(1)}(kr)$  is the Hankel function of the first kind,  $H_n^{(2)}(kr)$  is the Hankel function of second kind,  $k$  is the radial propagation constant of the radiation mode in air region,  $k_1$  and  $k_2$  are the radial propagation constants of the radiation modes in the core and cladding respectively.  $\beta$  is the longitudinal propagation constant of the radiation modes, which can be related to the radial propagation constants of the different regions through the following relation,

$$\beta^2 = k_c^2 - k_1^2 = k_d^2 - k_2^2 = k_0^2 - k^2 \quad (5)$$

The boundary conditions on the core-cladding interface as well as the cladding-air interface are applied to get a linear system of eight equations for the unknown coefficients in (1-4). As the equations are source-free, the problem of determining the radiation modes is an eigenvalue problem, where the values of  $\alpha_n$  corresponding to the different radiation modes are the eigenvalues of the problem. These eigenvalues can be obtained by setting the system determinant to zero, which leads to the following expression for the phase shifts of the different radiation modes

$$\alpha_n = \tan^{-1} \left[ \frac{-B_i \pm \sqrt{B_i^2 - 4A_i C_i}}{2A_i} \right] \quad (6)$$

where  $A_i, B_i$  and  $C_i$  are defined in appendix A.

The eigenvectors are then obtained by solving the system of equations for each eigenvalue.

It is clear, from (6), that for each value of  $n$ , there exist two values of  $\alpha_n$ . This implies the existence of two types of radiation modes: *EH* and *HE*.

### 2.1.1. Orthogonality of the radiation modes

The orthogonality between two modes  $p$  and  $q$ , propagating along an open waveguide can be expressed as [8]

$$\iint_{C.S.A} (\mathbf{E}_q \times \mathbf{H}_p) \cdot \mathbf{a}_z da = 0 \quad (7-a)$$

where,  $\alpha$  is the cross-sectional area of the waveguide. The cross product integral can be expressed as a contour integral [8, p417, 418] as follow

$$\iint_{C.S.A} (\mathbf{E}_q \times \mathbf{H}_p) \cdot \mathbf{a}_z da = \frac{1}{j(\beta^2 - \beta'^2)} \oint_C \left[ (E_{q\phi} H_{pz} - H_{qz} E_{p\phi}) + \beta' (E_{qz} H_{p\phi} - H_{q\phi} E_{pz}) \right] r d\phi \quad (7-b)$$

where,  $\beta$  and  $\beta'$  are the longitudinal propagation constants of the modes  $p$  and  $q$ , respectively. The closed contour,  $C$  is divided into separate closed contours each enclosing a sub-region of infinite cross section without crossing the interface between any two media of different dielectric constants as shown in Fig. 1. The integration over the straight paths of the contour,  $C$  will vanish since each pair of these paths are coincident and have opposite directions. Except for the outer circular contour,  $C_\infty$ , the

integration on the other circular contours vanishes due to coincidence of opposite paths and continuity of the field components on the sides of the interfaces.

Using (15-b), we can arrive at the following expression for the cross-sectional integral,

$$\iint_{c.s.A} (\mathbf{E}_q \times \mathbf{H}_p) \cdot \mathbf{a}_z d\alpha = -\frac{\pi\omega\mu(e_p^\alpha e_q^{\prime\alpha} \beta + h_p^\alpha h_q^{\prime\alpha} \beta') \cos(\alpha - \alpha')}{(kk')^{\frac{3}{2}}} \delta_{pq} \delta(k - k') \quad (8)$$

where  $\delta_{pq}$  is the Kronecker delta function and  $\delta(k - k')$  is the Dirac delta function. Thus the radiation modes are orthogonal to each other with respect to the mode order as well as the radial propagation constant. For two modes of the same order  $n$  and radial propagation constant  $k$ , referred previously as  $EH$  and  $HE$  modes, to be orthogonal, the following equation must be satisfied

$$e_n^\alpha e_n^{\prime\alpha} + h_n^\alpha h_n^{\prime\alpha} = 0 \quad (9)$$

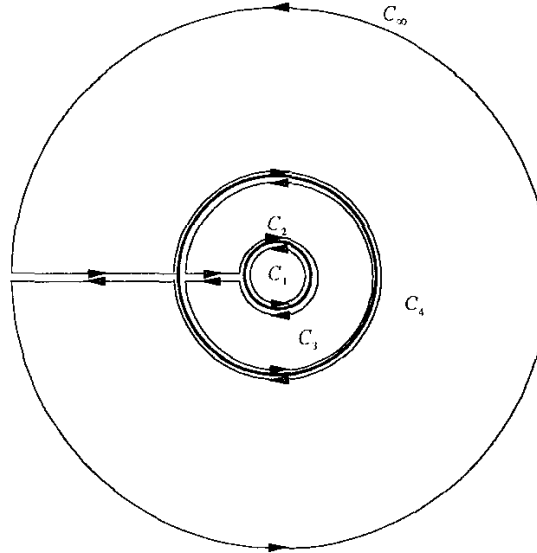


Fig. 1 Fiber cross section with the contours of each region

It's evident that a single mode can't satisfy the above condition, therefore a new set of orthogonal modes can be constructed such that each mode of this new set is a combination of the original  $EH$  and  $HE$  modes of the same order. Thus, a field of a mode belonging to the new set of modes can be expressed as

$$M_{new1} = M^{he} \quad (10-a)$$

$$M_{new2} = M^{he} + \mathcal{D}M^{eh} \quad (10-b)$$

where  $M^{he}$  and  $M^{eh}$  refer to the original nonorthogonal two modes,  $M_{new1}$  and  $M_{new2}$  are the new orthogonal modes,  $\mathcal{D}$  must satisfy the following condition

$$\mathcal{D} = -\frac{h_n^a h_n^{a\prime} + e_n^a e_n^{a\prime}}{[h_n^a h_n^{a\prime} + e_n^a e_n^{a\prime}] \cos(\alpha_n^{eh} - \alpha_n^{he})} \quad (11)$$



Although the modes of the continuous spectrum satisfy the optical fiber boundary conditions, none of them can actually be supported alone, since each mode contains an infinite amount of power. The total radiation field constitute a complete set of modes and can be represented as an integral of the fields of radiation modes over the radial propagation constant, which has normally a finite amount of power.

### 2.1.2. Normalization of the radiation modes

For the power content of the radiation mode to be unity, the value of the mode fields must be divided by a normalization factor. The normalization factors of the two types of radiation modes, expressed in (10) can be obtained using (7-b), to get

$$N_{c\_new1} = \frac{j}{k_0} \sqrt{\frac{\pi\eta_0 \tilde{\beta} \psi_{new1}}{\tilde{k}^3}} \quad (12-a)$$

$$N_{c\_new2} = \frac{j}{k_0} \sqrt{\frac{\pi\eta_0 \tilde{\beta} \psi_{new2}}{\tilde{k}^3}} \quad (12-b)$$

where

$$\psi_{new1} = \left[ h_n^{a\_he^2} + e_n^{a\_he^2} \right] \quad (13-a)$$

$$\psi_{new2} = 2\mathcal{D} \left[ h_n^{a\_he^2} h_n^{a\_eh} + e_n^{a\_he^2} e_n^{a\_eh} \right] \cos(\alpha_n^{eh} - \alpha_n^{he}) + \left[ h_n^{a\_he^2} + e_n^{a\_he^2} \right] + \mathcal{D}^2 \left[ h_n^{a\_eh^2} + e_n^{a\_eh^2} \right] \quad (13-b)$$

where  $\tilde{\beta}$  and  $\tilde{k}$  are normalized longitudinal and radial propagation constant.

In general, this set of radiation modes, together with the guided modes of the optical fiber can be used to solve longitudinal discontinuity problems along the fiber.

### 3. Power coupling between two step-index single-mode optical fiber sections with different refractive indices

In the following, the discontinuity occurring due to a joint between two sections of single-mode optical fiber with different refractive indices is treated using the mode-matching technique. The dominant mode is assumed to be propagating in the first section optical fiber and incident on the discontinuity plane. It is required to evaluate the power transferred to the second section of the optical fiber as well as the power loss due to the discontinuity. The total field in the first section optical fiber side is expressed as a summation of the incident and reflected guided waves and an integration of the reflected radiation modes with unknown reflection coefficients over the entire domain of radial propagation constant,  $k$ . The total field in the second section optical fiber is expressed as a summation of the transmitted guided wave and an integration of the transmitted radiation modes with unknown transmission coefficients over the entire domain of radial propagation constant,  $m$ . The reflection and the transmission coefficients of the different modes are obtained by matching the transverse fields on both sides of the plane of discontinuity,  $z = 0$ . Thus the total transverse fields in the two fiber sections can be expressed as,

$$\mathbf{e}_{t1} = \left( e^{-j\nu_1 z} + \Gamma_d e^{j\nu_1 z} \right) \mathbf{e}_{t1d} + \sum_{n=0}^{\infty} \int_0^{\infty} \left[ \Gamma_{\alpha_1}(k, n) \mathbf{e}_{t1\alpha_1}(k, n) + \Gamma_{\alpha_2}(k, n) \mathbf{e}_{t1\alpha_2}(k, n) \right] e^{j\beta z} dk. \quad (14-a)$$



$$\mathbf{h}_{11} = \left( e^{-j\nu_2 z} - \Gamma_d e^{j\nu_2 z} \right) \mathbf{h}_{11d} - \sum_{n=0}^{\infty} \int_0^{\infty} \left[ \Gamma_{\alpha_1}(k, n) \mathbf{h}_{11\alpha_1}(k, n) + \Gamma_{\alpha_2}(k, n) \mathbf{h}_{11\alpha_2}(k, n) \right] e^{j\beta z} dk. \quad (14-b)$$

$$\mathbf{e}_{12} = T_d e^{-j\nu_2 z} \mathbf{e}_{12d} + \sum_{n=0}^{\infty} \int_0^{\infty} \left[ T_{\alpha_1}(m, n) \mathbf{e}_{12\alpha_1}(m, n) + T_{\alpha_2}(m, n) \mathbf{e}_{12\alpha_2}(m, n) \right] e^{-j\sigma z} dm. \quad (15-a)$$

$$\mathbf{h}_{12} = T_d e^{-j\nu_2 z} \mathbf{h}_{12d} + \sum_{n=0}^{\infty} \int_0^{\infty} \left[ T_{\alpha_1}(m, n) \mathbf{h}_{12\alpha_1}(m, n) + T_{\alpha_2}(m, n) \mathbf{h}_{12\alpha_2}(m, n) \right] e^{-j\sigma z} dm. \quad (15-b)$$

where  $\mathbf{e}_{11d}$  and  $\mathbf{h}_{11d}$  are the transverse electric and magnetic fields of the guided mode in the first section,  $\mathbf{e}_{12d}$  and  $\mathbf{h}_{12d}$  are the transverse electric and magnetic fields of the guided mode in the second section,  $\mathbf{e}_{11\alpha_1}(k, n)$  and  $\mathbf{h}_{11\alpha_1}(k, n)$  are the transverse electric and magnetic fields of the first type radiation mode in the first section,  $\mathbf{e}_{12\alpha_1}(m, n)$  and  $\mathbf{h}_{12\alpha_1}(m, n)$  are the transverse electric and magnetic fields of the first type radiation modes in the second section,  $\mathbf{e}_{11\alpha_2}(k, n)$  and  $\mathbf{h}_{11\alpha_2}(k, n)$  are the transverse electric and magnetic fields of the second type radiation modes in the first section,  $\mathbf{e}_{12\alpha_2}(m, n)$  and  $\mathbf{h}_{12\alpha_2}(m, n)$  are the transverse electric and magnetic fields of the second type radiation modes in the second section,  $m$  and  $k$  are the radial propagation constants of the radiation modes in the first and second sections respectively,  $\nu_1$  and  $\nu_2$  are the longitudinal propagation constants of the guided modes of the first and second sections respectively,  $\Gamma_d$  is the reflection coefficient of the guided mode.  $\Gamma_{\alpha_1}(k, n)$  and  $\Gamma_{\alpha_2}(k, n)$  are the reflection coefficients of the two types of radiation modes.  $T_{\alpha_1}(m, n)$  and  $T_{\alpha_2}(m, n)$  are the transmission coefficients of the two types of radiation modes.

By matching the transverse electric field on both sides of the discontinuity plane,  $z = 0$ , the following equation is obtained:

$$\begin{aligned} (1 + \Gamma_d) \mathbf{e}_{11d} + \sum_{n=0}^{\infty} \int_0^{\infty} \left[ \Gamma_{\alpha_1}(k, n) \mathbf{e}_{11\alpha_1}(k, n) + \Gamma_{\alpha_2}(k, n) \mathbf{e}_{11\alpha_2}(k, n) \right] dk \\ = T_d \mathbf{e}_{12d} + \sum_{n=0}^{\infty} \int_0^{\infty} \left[ T_{\alpha_1}(m, n) \mathbf{e}_{12\alpha_1}(m, n) + T_{\alpha_2}(m, n) \mathbf{e}_{12\alpha_2}(m, n) \right] dm \quad (16) \end{aligned}$$

By matching the transverse magnetic field on both sides of the discontinuity, plane  $Z = 0$ , the following equation is obtained:

$$\begin{aligned} (1 - \Gamma_d) \mathbf{h}_{11d} - \sum_{n=0}^{\infty} \int_0^{\infty} \left[ \Gamma_{\alpha_1}(k, n) \mathbf{h}_{11\alpha_1}(k, n) + \Gamma_{\alpha_2}(k, n) \mathbf{h}_{11\alpha_2}(k, n) \right] dk \\ = T_d \mathbf{h}_{12d} + \sum_{n=0}^{\infty} \int_0^{\infty} \left[ T_{\alpha_1}(m, n) \mathbf{h}_{12\alpha_1}(m, n) + T_{\alpha_2}(m, n) \mathbf{h}_{12\alpha_2}(m, n) \right] dm \quad (17) \end{aligned}$$

Modes orthogonality can be employed to construct a system of integral equations for the unknown modes amplitudes find the equations for the unknown mode amplitudes. The modes orthogonality for the modes of the second optical fiber section is utilized through the following procedure. First a cross product operation is carried out between (16) and the magnetic fields,  $\mathbf{h}_{t2d}$ ,  $\mathbf{h}_{t2\alpha_1}(M)$ , and  $\mathbf{h}_{t2\alpha_2}(M)$ . Second a cross product operation is carried out between (17) by  $\mathbf{e}_{t2d}$ ,  $\mathbf{e}_{t2\alpha_1}(M)$ , and  $\mathbf{e}_{t2\alpha_2}(M)$ , where,  $M$  refers to certain value of  $m$ . Then adding and subtracting each pair, of the six resulting equations, concerned with the same unknown, one gets the following relations

$$2T_{\alpha_1}(M) = C_{t1d\_t2\alpha 1}^{M'} + \Gamma_d C_{t1d\_t2\alpha 1}^M + \int_0^\infty \left[ \Gamma_{\alpha_1}(k) C_{t1\alpha 1\_t2\alpha 1}^{kM} + \Gamma_{\alpha_2}(k) C_{\alpha 2_{t1,\alpha 1}t2}^{kM} \right] dk \quad (18-a)$$

$$2T_d = C_{t1d\_t2d}^+ + \Gamma_d C_{t1d\_t2d}^- + \int_0^\infty \left[ \Gamma_{\alpha_1}(k) C_{t1\alpha 1\_t2d}^k + \Gamma_{\alpha_2}(k) C_{t1\alpha 2\_t2d}^k \right] dk \quad (18-b)$$

$$2T_{\alpha_2}(M) = C_{t1d\_t2\alpha 2}^M + \Gamma_d C_{t1d\_t2\alpha 2}^- + \int_0^\infty \left[ \Gamma_{\alpha_1}(k) C_{t1\alpha 1\_t2\alpha 2}^{kM} + \Gamma_{\alpha_2}(k) C_{t1\alpha 2\_t2\alpha 2}^{kM} \right] dk \quad (18-c)$$

$$0 = C_{t1d\_t2d}^- + \Gamma_d C_{t1d\_t2d}^+ + \int_0^\infty \left[ \Gamma_{\alpha_1}(k) C_{t1\alpha 1\_t2d}^k + \Gamma_{\alpha_2}(k) C_{t1\alpha 2\_t2d}^k \right] dk \quad (18-d)$$

$$0 = C_{t1d\_t2\alpha 1}^M + \Gamma_d C_{t1d\_t2\alpha 1}^+ + \int_0^\infty \left[ \Gamma_{\alpha_1}(k) C_{t1\alpha 1\_t2\alpha 1}^{kM} + \Gamma_{\alpha_2}(k) C_{t1\alpha 2\_t2\alpha 1}^{kM} \right] dk \quad (18-e)$$

$$0 = C_{t1d\_t2\alpha 2}^M + \Gamma_d C_{t1d\_t2\alpha 2}^+ + \int_0^\infty \left[ \Gamma_{\alpha_1}(k) C_{t1\alpha 1\_t2\alpha 2}^{kM} + \Gamma_{\alpha_2}(k) C_{t1\alpha 2\_t2\alpha 2}^{kM} \right] dk \quad (18-f)$$

where

$$C_{t1d\_t2d}^\mp = \iint_{C.S.A} (e_{t1d} \times h_{t2d} \mp e_{t2d} \times h_{t1d}) \cdot da \quad (19-a)$$

$$C_{t1d\_t2\alpha}^{M\mp} = \iint_{C.S.A} (e_{t1d} \times h_{t2\alpha}(M) \mp e_{t2\alpha}(M) \times h_{t1d}) \cdot da \quad (19-b)$$

$$C_{t1\alpha\_t2\alpha}^{km\mp} = \iint_{C.S.A} (e_{t1\alpha}(k) \times h_{t2\alpha}(m) \mp e_{t2\alpha}(m) \times h_{t1\alpha}(m)) \cdot da \quad (19-c)$$

The quantities in (19) can be evaluated with the aid of the following expression [6],

$$\iint_{C.S.A} (\bar{e}_q \times \bar{h}_p \mp \bar{e}_p \times \bar{h}_q) \cdot \bar{a}_z da$$

$$= \frac{1}{j(\beta_p \pm \beta_q)} \left[ \oint_C (\bar{h}_q^\pm \times \bar{e}_p + \bar{e}_q^\pm \times \bar{h}_p) \cdot \bar{a}_r dl - j\omega(\epsilon_q - \epsilon_p) \iint_{C.S.A} \bar{e}_q^\pm \cdot \bar{e}_p da \right] \quad (20)$$

where the superscripts , +, and . -, refers to waves propagating in +ve and -ve z- directions respectively and  $C$  is the contour defined in Fig. 1.

Using (20), the surface integral on the left hand side can be expressed as a contour integral and a surface integral. It should be noticed that due to the factor  $(\varepsilon_q - \varepsilon_p)$ , the term including the surface integral on the right hand side vanishes for all parts of the cross-sectional area shared between two regions of the same relative permativity. The contour integral is carried out along the circular path at infinity as explained before.

It can be shown that, after carrying out the integration in (19-c), the kernel coefficients take the following form

$$C_{t1\alpha_- t2\alpha}^{km+} = \frac{f(k, m)}{k - m} + y(k, m)\delta(k - m) \quad (21)$$

where,  $f(k, m)$  and  $y(k, m)$  are functions of both  $k$  and  $m$ , and can be obtained by carrying out the surface integration in (19-c).

Due to the existence of the quantity  $(k - m)$  in the denominator of (21), the kernel coefficients in (18-e) and (18-f) are singular where, the singularity occurs due to the presence of two radiation modes belonging to different fiber sections and having the same propagation constant, i.e.  $k = m$ . Hence, equations (18) constitute a system of singular integral equations

### 3.1. Solution of the system of singular integral equations

The solution of the unknown reflection and transmission coefficients of (18) can be obtained through the conversion of the system of the singular integral equations, (18), into a finite system of linear equations. This is achieved by expanding the unknown transmission and reflection coefficients of the radiation modes as a series of pulse functions with unknown amplitudes over the domain of interest, which define the radiation modes:  $0 \leq \tilde{k} \leq 1$ . This domain is divided into a number of sub-domains such that the singular point, if exists, lies exactly at the middle point of a sub-domain. The number of the sub-domains is taken large enough to get accurate results. Thus the unknown reflection and transmission coefficients can be expanded as

$$\Gamma_{\alpha_{1,2}}(k) = \sum_{i=1}^N \Gamma_{\alpha_{1,2}}^i \left[ u \left( k - \left( k_i - \frac{\Delta}{2} \right) \right) - u \left( k - \left( k_i + \frac{\Delta}{2} \right) \right) \right] \quad (22-a)$$

$$T_{\alpha_{1,2}}(k) = \sum_{i=1}^N T_{\alpha_{1,2}}^i \left[ u \left( k - \left( k_i - \frac{\Delta}{2} \right) \right) - u \left( k - \left( k_i + \frac{\Delta}{2} \right) \right) \right] \quad (22-b)$$

where,  $\Gamma_{\alpha_{1,2}}^i$  and  $T_{\alpha_{1,2}}^i$  are the unknown weights of the pulse expansion functions of the reflection and transmission coefficients, respectively,  $N$  is the number of sub-domains, and  $u$  is the unit step function. After employing (22), the obtained linear system of equations can be solved by exact numerical techniques.

### 3.2. Power balance

For the sake of verifying the validity of the obtained solutions for the reflected and transmitted fields, the power balance is investigated. The power balance requires that the incident power equals the summation of the reflected and transmitted power. This can be expressed as

$$P_{inc} = P_s \quad (23-a)$$

where  $P_s$  is the scattered power, which is defined as

$$P_s = P_{rg} + P_{rc} + P_{tc} + P_{tg} \quad (23-b)$$



where  $P_{inc}$  is the power of the dominant mode incident on the plane of discontinuity,  $P_{rg}$  is the power of the reflected guided mode,  $P_{tg}$  is the power of the transmitted guided mode,  $P_{rc}$  is the power of the reflected radiation modes, and  $P_{tc}$  is the power of the transmitted radiation modes.

#### 4. Numerical results and discussion

In this section, the reflection and transmission coefficients for the different modes are calculated. Also the coupled power as well as the radiation power due to discontinuity between two optical fiber sections are evaluated and presented for different values of refractive index of the second fiber section.

It should be noted that the numerical results presented in the following discussion considering fiber sections with the following parameters unless otherwise indicated,  $b = 125 \mu\text{m}$ ,  $\lambda = 1.3 \mu\text{m}$ , and  $n_{d1} = n_{d2} = 1.4993$ .

Fig. 2 shows sample plots for the singular kernels of the singular integral equations (18-e) and (18-f). It's clear that these singular kernels are almost zero in the entire domain of integration except for narrow regions around the singular points. This means that the discretization operation, carried out to convert the integrals in (18) to finite summations as described in section (3.1), will result in a finite linear system whose matrix is quasi-diagonal. This simplifies and speeds up the numerical process of solving this system.

The numerical solution of the obtained linear system of equations gives rise to the values of the reflection and transmission coefficients of the different modes. Considering fiber sections with the parameters indicated above, this numerical solution results in a very low value of the reflection coefficient of the guided mode, that is  $\Gamma_d = -0.0432$  and a large value of the transmission coefficient of the guided mode, that is  $T_d = 0.9938$ . By using (35-a) and (35-b) the values of the power transmitted to the second section and that reflected back to the first section are,  $P_{tg} = 0.9876$  and  $P_{rg} = 0.0019$ , respectively. It can be concluded that because of the small difference between  $n_{c1}$  and  $n_{c2}$ , most of the incident power transfer to the second section whereas a little a little amount of the power is reflected back to the first section.

Fig. 3 shows plots for the reflection and the transmission coefficients of the radiation modes as functions of the radial propagation constant. It's seen in the figure that the reflection coefficients  $\Gamma_{\alpha 1}$  and  $\Gamma_{\alpha 2}$  of the radiation modes have peaks at,  $\tilde{k} \approx 0.114$ . Also the transmission coefficients  $T_{\alpha 1}$  and  $T_{\alpha 2}$  of the radiation modes have peaks at,  $\tilde{m} \approx 0.22$ . The values of the radial propagation constant at which the reflection or transmission coefficients have peaks identifies the maximum directions, and can be related to the directions of the optical rays in the corresponding fiber section.

According to equations (35-c) and (35-d), the power carried by the reflected and transmitted radiation modes are  $P_{rc} = 0.0002$  and  $P_{tc} = 0.0042$  respectively. According to (34) the scattered power is  $P_s = 0.994$ . Thus the total power of the scattered field is nearly equal to the power of the incident mode (unity), which reflects the validity of the applied methods and the accuracy of the obtained results.

Other cases considering various values of  $n_{c2}$  are shown in Table 1. It's shown in the table that in the case of matched fiber sections, i.e.  $n_{c1} = n_{c2}$ , the incident power is completely transmitted to the second fiber section.

Fig. 4 shows a plot for the optical power coupled to the second fiber section against the refractive index of the second optical fiber section,  $n_{c2}$ . It's clear that the incident power is totally

coupled to the second fiber section when the optical fiber sections have the same values of the refractive indices. It's seen in the figure that as the refractive index of the second fiber section is deviated from that of the first fiber section the transferred power is significantly decreased.

Fig. 5 shows a plot for the total power loss, which is the summation of the  $P_{rg}$ ,  $P_{rc}$ , and  $P_{lc}$  against  $n_{c2}$ . It's clear that no power loss occurs in the case of matched fiber sections. It's also seen that the power loss increases as the refractive index of the second fiber section is deviated from that of the first fiber section.

Other case considering fiber sections with core radius  $a = 5 \mu\text{m}$ , which refers to high frequency case, and core refractive index  $n_{c1} = 1.502586$  is evaluated with various values of  $n_{c2}$  in table 2.

Fig. 6 and Fig. 7 shows a plot for the optical power coupled to the second fiber section and the total power loss against the refractive index of the second optical fiber section,  $n_{c2}$ , respectively for the previous case.

$n_{c2}$	$P_{rg}$	$P_{lg}$	$P_{rc}$	$P_{lc}$
1.9331	0.001863	0.987607	0.000181	0.004187
1.900028	0.000594	0.995589	0.000165	0.0023255
1.8368	0	1	0	0
1.777580	0.000004	0.993064	0.000106	0.0035481
1.749653	0.000267	0.978715	0.000295	0.009905
1.722907	0.0021828	0.955592	0.028613	0.0005643
1.6974	0.008136	0.920696	0.001008	0.0593736
1.5904	0.237842	0.42393	0.008976	0.0977557

Table 1. Power carried by different types of modes for different values of  $n_{c2}$  for  $a = 0.39 \mu\text{m}$  and  $n_{c1} = 1.8368$

$n_{c2}$	$P_{rg}$	$P_{lg}$	$P_{rc}$	$P_{lc}$
1.5021	2e-8	0.99964	1.6e-10	3.5e-9
1.5016	7e-8	0.9928	5e-10	1.3e-8
1.501	2e-7	0.964	1.6e-9	1.24e-7
1.5006	2.3e-7	0.85	2.4e-9	5.1e-8

Table 2. Power carried by different types of modes for different values of  $n_{c2}$  for  $a = 5 \mu\text{m}$  and  $n_{c1} = 1.502586$

## 5. Conclusion

Employing the complete spectrum of modes of a step-index optical fiber, the application of the mode matching technique on the problem of a step discontinuity between two optical fiber sections of different refractive indices leads to a system of singular integral equations. The singular kernels of integral equations are not zero for the different values of the radial propagation constant except for very narrow intervals around the singular points. This behavior of singular kernels enables fast and efficient numerical solution of the system of singular integral equations to get the excitation coefficients of the different modes in the two fiber sections. The power coupled to the second fiber section as well as the power loss due to the discontinuity are found to be strongly dependent on the difference of the refractive indices of the two fiber sections. As the refractive indices are more deviated from each other, the transmitted power is decreased whereas the power loss is increased and vice versa. The power balance is

investigated where the power of the incident mode is found equal to the summation of the reflected and radiated power together with that coupled to the second fiber section, which reflects the validity of the applied method and the accuracy of the obtained results. Optical fiber sections with quite arbitrary values of core radius are investigated showing that the mode matching technique as well as the method of solving the system of singular integral equations as employed in this paper are completely frequency independent.

### Appendix A

The following expressions are definitions for the symbols appearing in equations (13) and (14)

$$A_i = Y_n'^2(kb)\bar{A} + kY_n(kb)Y_n'(kb)\bar{B} + k^2Y_n^2(kb)\bar{C} \quad (A-1)$$

$$B_i = -2J_n'(kb)Y_n'(kb)\bar{A} - (J_n(kb)Y_n'(kb) + J_n'(kb)Y_n(kb))k\bar{B} - 2k^2J_n(kb)Y_n(kb)\bar{C} \quad (A-2)$$

$$C_i = J_n'^2(kb)\bar{A} + kJ_n(kb)J_n'(kb)\bar{B} + k^2J_n^2(kb)\bar{C} \quad (A-3)$$

And

$$\bar{A} = (\omega^2 \mu \eta_d \varepsilon_a) [A_{21}Y_n^2(k_2b) + (A_{22} + A_{23})J_n(k_2b)Y_n(k_2b) + A_{24}J_n^2(k_2b)] \quad (A-4)$$

$$\bar{C} = C_0 + C_1 + C_2 \quad (A-5)$$

$$\bar{B} = \left( \frac{-\omega^2 \mu \eta_d}{k_2} \right) \left[ \begin{aligned} & [\varepsilon_d + \varepsilon_a] [A_{21}Y_n(k_2b)Y_n'(k_2b) + A_{24}J_n(k_2b)J_n'(k_2b)] \\ & + [(\varepsilon_d A_{22} + \varepsilon_a A_{23})J_n(k_2b)Y_n'(k_2b) + (\varepsilon_a A_{22} + \varepsilon_d A_{23})J_n'(k_2b)Y_n(k_2b)] \end{aligned} \right] \quad (A-6)$$

$$C_2 = \left( \frac{\omega^2 \mu \eta_d \varepsilon_d}{k_2^2} \right) [A_{21}Y_n^2(k_2b) + (A_{22} + A_{23})J_n'(k_2b)Y_n'(k_2b) + A_{24}J_n'^2(k_2b)] \quad (A-7)$$

$$C_1 = \frac{\eta_d V_n U_n \omega \mu}{k_2} [S_n J_n(k_2a) - Y_n(k_2a)R_n] [Y_n(k_2b)J_n'(k_2b) - J_n(k_2b)Y_n'(k_2b)] \\ + \frac{\eta_d^2 V_n U_n \omega \varepsilon_d}{k_2} [M_n J_n(k_2a) - L_n Y_n(k_2a)] [Y_n(k_2b)J_n'(k_2b) - J_n(k_2b)Y_n'(k_2b)] \quad (A-8)$$

$$C_0 = \eta_d^2 V_n^2 U_n^2 [Y_n(k_2a)J_n(k_2b) - J_n(k_2a)Y_n(k_2b)] [J_n(k_2a)Y_n(k_2b) - Y_n(k_2a)J_n(k_2b)] \\ + \eta_d U_n^2 [L_n R_n Y_n^2(k_2b) + M_n S_n J_n^2(k_2b) - J_n(k_2b)Y_n(k_2b)] [L_n S_n + M_n R_n] \quad (A-9)$$

$$A_{21} = \eta_d J_n^2(k_2a) V_n^2 - L_n R_n \quad (A-10)$$

$$A_{22} = M_n R_n - \eta_d J_n(k_2a) V_n^2 Y_n(k_2a) \quad (A-11)$$

$$A_{23} = L_n S_n - \eta_d Y_n(k_2a) V_n^2 J_n(k_2a) \quad (A-12)$$

$$A_{24} = \eta_d Y_n^2(k_2a) V_n^2 - M_n S_n \quad (A-13)$$

$$V_n = \frac{n\beta}{a} \left[ \frac{1}{k_1^2} - \frac{1}{k_2^2} \right] \quad (A-14)$$

$$U_n = \frac{n\beta}{b} \left[ \frac{1}{k_2^2} - \frac{1}{k^2} \right] \quad (A-15)$$

$$L_n = \omega \mu J_n(k_2a) \left[ \frac{J_n'(k_1a)}{k_1 J_n(k_1a)} - \frac{J_n'(k_2a)}{k_2 J_n(k_2a)} \right] \quad (A-16)$$

$$M_n = \omega \mu Y_n(k_2a) \left[ \frac{J_n'(k_1a)}{k_1 J_n(k_1a)} - \frac{Y_n'(k_2a)}{k_2 Y_n(k_2a)} \right] \quad (A-17)$$

$$N_n = \varpi \mu J_n(k_2 b) \left[ \frac{J'_n(k_2 b)}{k_2 J_n(k_2 b)} - \frac{W'_n(kb, \alpha_n)}{kW_n(kb, \alpha_n)} \right] \quad (\text{A-18})$$

$$Z_n = \varpi \mu Y_n(k_2 b) \left[ \frac{Y'_n(k_2 b)}{k_2 Y_n(k_2 b)} - \frac{W'_n(kb, \alpha_n)}{kW_n(kb, \alpha_n)} \right] \quad (\text{A-19})$$

$$R_n = \varpi \eta_d J_n(k_2 a) \left[ \varepsilon_c \frac{J'_n(k_1 a)}{k_1 J_n(k_1 a)} - \varepsilon_d \frac{J'_n(k_2 a)}{k_2 J_n(k_2 a)} \right] \quad (\text{A-20})$$

$$S_n = \varpi \eta_d Y_n(k_2 a) \left[ \varepsilon_c \frac{J'_n(k_1 a)}{k_1 J_n(k_1 a)} - \varepsilon_d \frac{Y'_n(k_2 a)}{k_2 Y_n(k_2 a)} \right] \quad (\text{A-21})$$

$$T_n = \varpi \eta_d J_n(k_2 b) \left[ \varepsilon_d \frac{J'_n(k_2 b)}{k_2 J_n(k_2 b)} - \varepsilon_a \frac{W'_n(kb, \alpha_n)}{kW_n(kb, \alpha_n)} \right] \quad (\text{A-22})$$

$$X_n = \varpi \eta_d Y_n(k_2 b) \left[ \varepsilon_d \frac{Y'_n(k_2 b)}{k_2 Y_n(k_2 b)} - \varepsilon_a \frac{W'_n(kb, \alpha_n)}{kW_n(kb, \alpha_n)} \right] \quad (\text{A-23})$$

$$\mathfrak{I}^{TE} = \frac{L_0 Y'_0(k_2 b) - M_0 J'_0(k_2 b)}{k_2} \quad (\text{A-24})$$

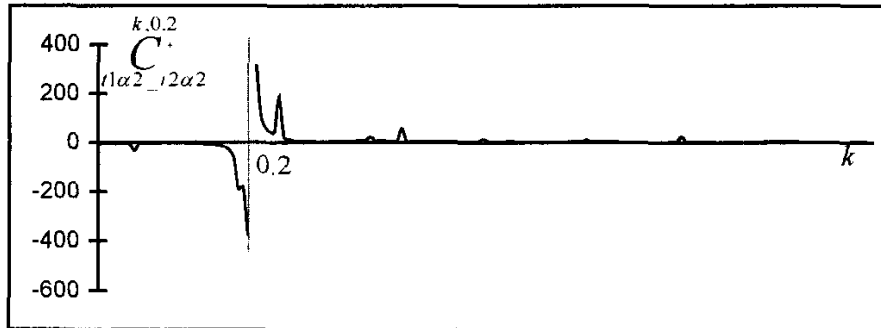
$$\mathfrak{R}^{TE} = \frac{M_0 J_0(k_2 b) - L_0 Y_0(k_2 b)}{k} \quad (\text{A-25})$$

$$\mathfrak{I}^{TM} = \varepsilon_d \left( \frac{S_0 J'_0(k_2 b) - R_0 Y'_0(k_2 b)}{k_2} \right) \quad (\text{A-26})$$

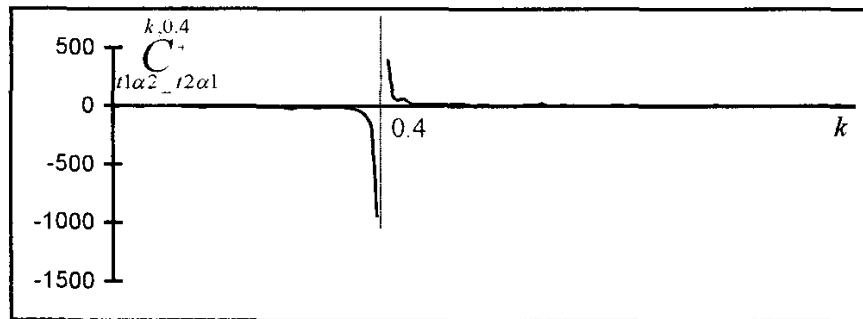
$$\mathfrak{R}^{TM} = \varepsilon_a \left( \frac{R_0 Y_0(k_2 b) - S_0 J_0(k_2 b)}{k} \right) \quad (\text{A-27})$$

### References

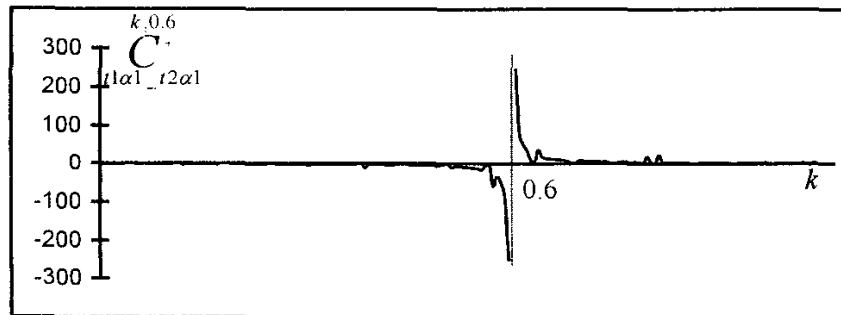
- [1] G. Keiser, "Optical Fiber Communications", McGraw-Hill Inc., London, 1974.
- [2] D. Marcuse, "Theory of Dielectric Optical Waveguides", Academic Press, New York and London, 1974
- [3] A. W. Snyder and J. D. Love, "Optical Waveguide Theory", The Institute of Advanced Studies, Australian National University, Canberra, Australia 1983.
- [4] D. Marcuse, "Light Transmission Optics", Van Nostrand Reinhold Company, Bell Telephone Laboratories, New York, 1982
- [5] G. Rozzi and M. Mongirado, "Open Electromagnetic Waveguides", The Institute of Electrical Engineers, London, United Kingdom, 1997.
- [6] E. L. Alwany, "Leaky Waves Antenna", M.Sc. Thesis, Al-Azhar University, Faculty of Engineering, 1980.
- [7] K. Hussein, "Radiation and Scattering of Electromagnetic Waves from Longitudinal Slot or Strip on Coaxial Structure", Ph.D Thesis, Cairo University, Faculty of Engineering, 2000.
- [8] R. Collin, "Field Theory of Guided Waves", Edition 2, IEEE Press, New York, 1990.



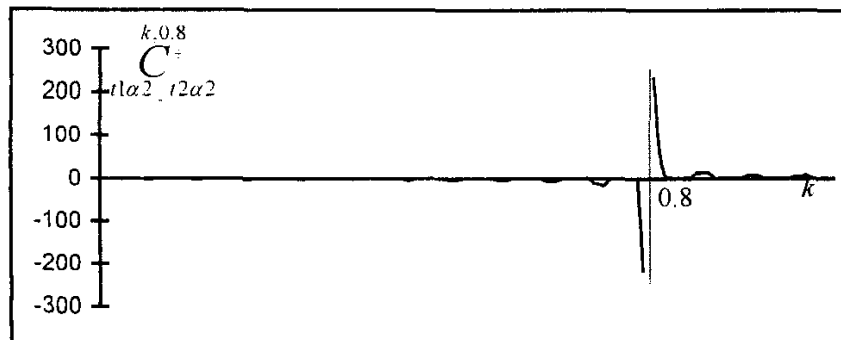
(a)  $m = 0.2$



(b)  $m = 0.4$

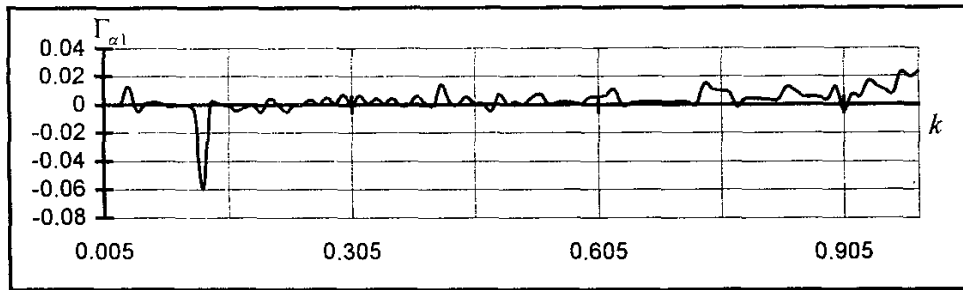


(c)  $m = 0.6$

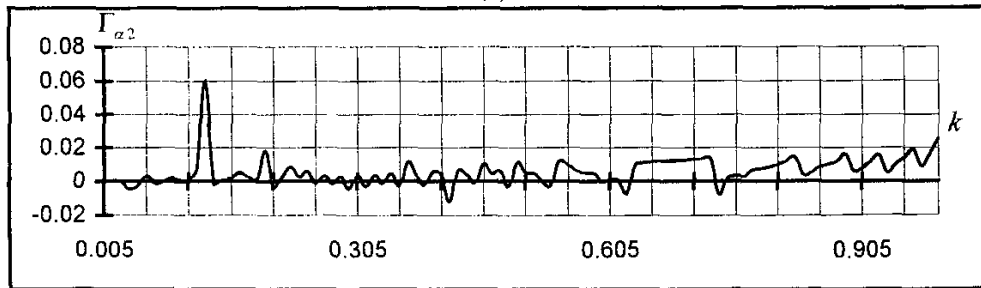


(d)  $m = 0.8$

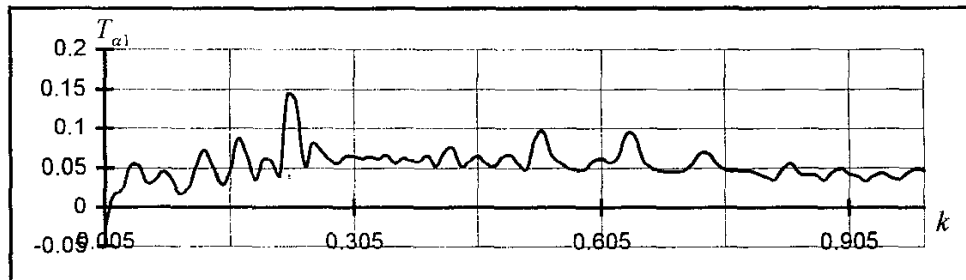
Fig. 2. Sample plots for singular kernel coefficients against the radial propagation constant



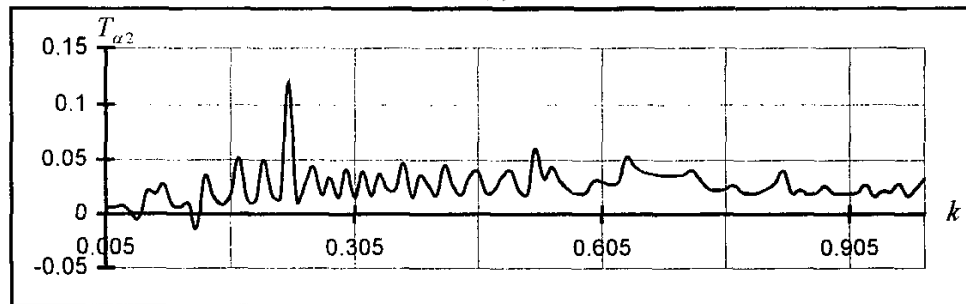
(a)



(b)



(c)



(d)

Fig. 3 Reflection and transmission coefficients of the radiation modes as functions of the radial propagation constant

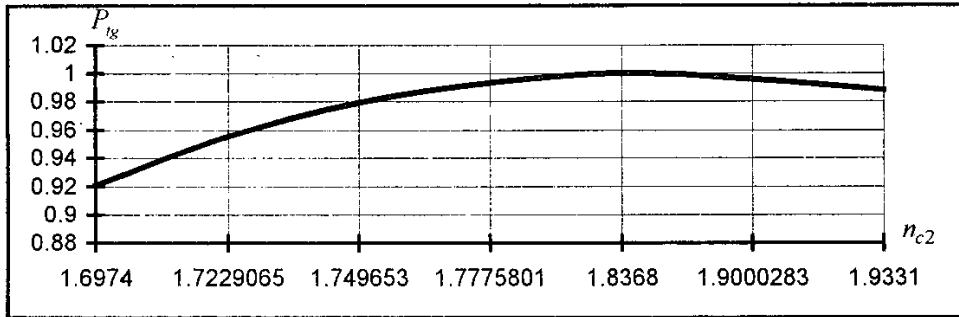


Fig. 4 The power coupled to the second fiber section as a function of  $n_{c2}$  at  $a = 0.39 \mu\text{m}$

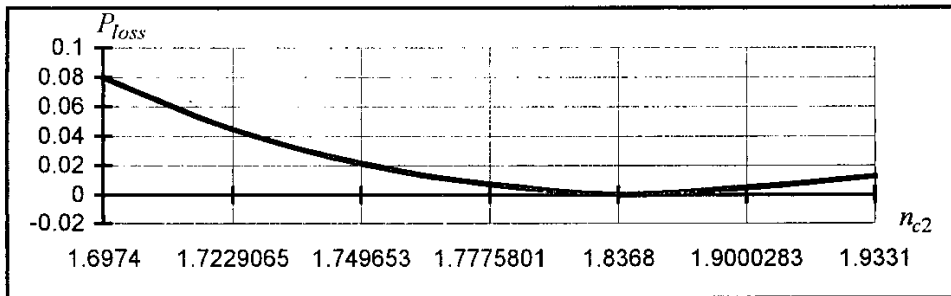


Fig. 5 The total power loss (reflected and radiated) as a function of  $n_{c2}$  at  $a = 0.39 \mu\text{m}$

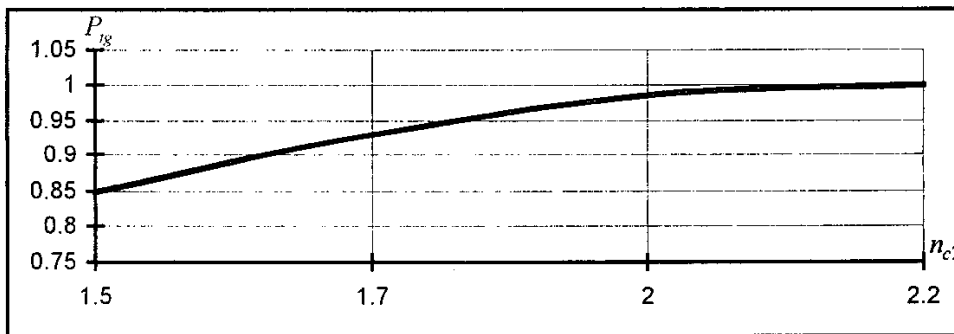


Fig. 6 The power coupled to the second fiber section as a function of  $n_{c2}$  at  $a = 5 \mu\text{m}$

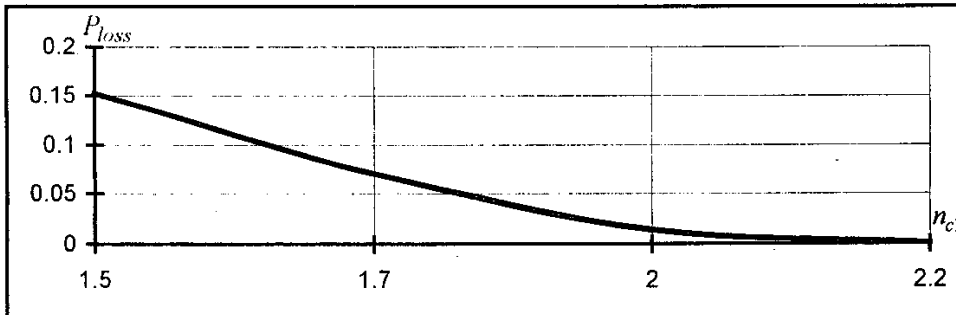


Fig. 7 The total power loss (reflected and radiated) as a function of  $n_{c2}$  at  $a = 5 \mu\text{m}$